

# The Electroabsorption-Modulated Laser as Optical Transmitter and Receiver: Status and Opportunities

Bernhard Schrenk\*

Center for Digital Safety&Security, AIT Austrian Institute of Technology, Giefinggasse 4, 1210 Vienna, Austria

\*[bernhard.schrenk@ait.ac.at](mailto:bernhard.schrenk@ait.ac.at)

**Abstract:** The rapid growth of digital services has led to a widespread deployment of opto-electronics that furnish the Internet as an efficient communication backbone. The electroabsorption-modulated laser (EML) is a representative example of a monolithic integrated electro-optic converter that has early become a commodity: It has been widely adopted in telecommunication networks in virtue of its cost- and energy-efficient light generation and modulation. This paper reviews the state-of-the-art of EML applications. Despite its simplicity, the EML addresses numerous use cases that require either the transmission or the reception of optical signals, such as equalizer-free high-bandwidth intensity-modulation / direct-detection links at low signal drive, analogue signal transmission with high signal integrity, spectral sculpting for dispersion-tolerant transmission, and vector modulation. Full-duplex transceiver functionality in lieu of a pair of dedicated half-duplex sub-systems is eventually attained by combining transmission and reception. This strategy of significantly reducing the cost for a bidirectional communication engine will be discussed for coherent digital data and analogue radio-over-fibre transmission, and optical ranging. The maturity of EMLs as coherent transceivers will be evidenced by a small penalty for realizing full-duplex transmission and the accomplishment of homodyne detection, which obviates digital signal processing for the purpose of signal recovery.

## 1. Introduction

The roll-out of vigorously flourishing digital services and applications has led to the seamless development of a high-capacity infrastructure that spans from short-reach to long-haul networks. This backbone of the Information Age has ever been able to keep pace with the demanding requirements of emerging applications. This never-ending process of winding each other up has consistently repeated itself over the past decades. Voice has been replaced by data as the main propeller that erodes available network capacity, followed by video and machine-to-machine communication. This impressive evolution is accompanied by a strong growth in traffic. Studies [1] have reported a compound annual growth rate of 60% in the long-haul segment and in global mobile traffic during the past years. Video upload has soared up at a 70% growth, while video streaming is currently growing at 50%. Data processing and caching in dedicated datacentres with more than 100,000 servers [2] necessitates intra-datacentre capacities surpassing 10 Pb/s, concentrated in a single spot of the modern cloud infrastructure.

These relentlessly expanding numbers highlight the importance of highly-effective transceiver sub-systems. It is found that technologies for the generation and processing of data follows a ~60% growth rate, while that supporting the transport of data is lagging behind at a ~20% rate [1]. A capacity crunch in the optical network infrastructure can only be mitigated by deploying high-capacity links. Considerable effort has been put in scaling up the spectral efficiency of optical networks through advanced modulation, in order to unleash the massive link capacities sought for [3]. However, further disruptive performance scaling is often prevented through capacity-reach trade-offs, which have led to a slow-down in per-link capacity growth and a

reconsideration towards a more parallel implementation approach, referred to as inverse multiplexing [4]. This approach roots on furnishing the network infrastructure with greatly simplified and thus cost- and energy-effective transmitter and receiver sub-systems.

Laser devices in the form of optical sources with co-integrated electro-optic modulators fit within a low-cost envelope and have been widely adopted in telecom and datacom systems. A prominent candidate for such an optical transmitter is the electroabsorption-modulated laser (EML). Its attractiveness for many applications domains, reaching from intra-datacentre and short-reach interconnects, fixed access and wireless fronthaul links, to metro-core networks, grounds on its potential to realize optical light generation and modulation in a monolithic fashion [5]. EMLs enjoy advantages such as small size and large bandwidths, combined with low driving requirements. As a matter of fact, the EML is an outstanding example of an early photonic integrated circuit with commercial success story, which has been recognized by leading scientists in the field, describing the EML as “arguably the most successful InP photonic integrated circuit” [6].

This paper aims to review the applications of EML technology under the umbrella of optical communications, spanning from use cases as optical transmitter and receiver to transceiver functionality (Fig. 1). The content of the paper is organized as follows. Section 2 introduces the foundations of the EML as transmitter, for which various applications aiming at digital and analogue signal transmission are discussed in Section 3, including advanced concepts such as spectral sculpting and vector modulation. Section 4 elaborates on the capabilities of the EML to serve direct and coherent detection. Towards the direction of the latter, polarisation-insensitive and coherent homodyne reception is explored. Section 5 highlights application-specific

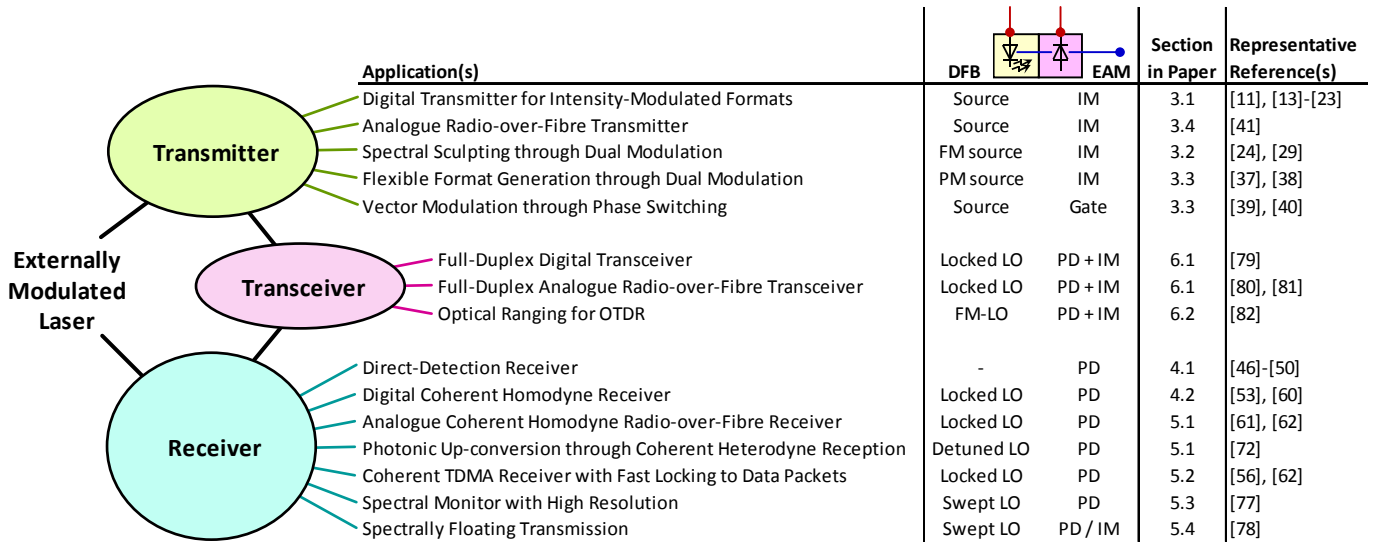


Fig. 1. Applications of EMLs as transmitter, receiver and transceiver. (IM ... intensity modulator, PD ... photodetector, FM ... frequency-modulated, PM ... phase-modulated.)

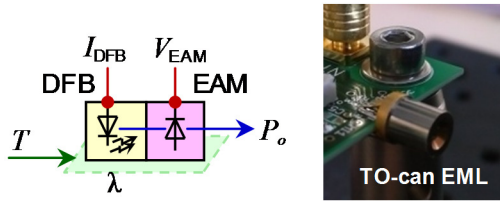


Fig. 2. The EML as compact and cost-energy-efficient transmitter.

challenges associated to coherent reception with an EML and includes analogue radio-over-fibre transmission, the packet-oriented reception with short guard time, spectral monitoring and wavelength-swept homodyne signal transmission. Section 6 takes the leap towards full-duplex signal transmission, for which a single EML simultaneously serves as transmitter and coherent receiver. Applications such as full-duplex analogue signal transmission and integrated optical ranging will be discussed. Finally, section 7 concludes the paper.

## 2. The EML as Optical Transmitter

EMLs sequentially combine optical light generation and modulation by means of monolithic integration. For this purpose, such an integrated laser modulator essentially consists of a distributed feedback (DFB) laser section and an electro-absorption modulator (EAM), as sketched in Fig. 2. Both elements can be integrated at small form-factor, to which DFB and EAM contribute with typical longitudinal dimensions of 350 and 75  $\mu\text{m}$ , respectively. Compared to alternative modulators schemes such as interferometric Mach-Zehnder arrangements, a high fabrication is yielded for EMLs.

The DFB laser launches a continuous-wave emission at wavelength  $\lambda$ , with a typical output power  $P_o$  of 10 dBm. Typical voltage-light-current (VLI) characteristics are presented in Fig. 3(a). Experimental data for V-I ( $\blacktriangle$ ) and L-I ( $\bullet$ ) of a transistor-outline EML is shown together with a

diode-based V-I model with differential resistance  $R_S$  and a linearly ramping L-I model above the threshold current  $I_{th}$ ,

$$V_{DFB} = V_J \ln \left( \frac{I_{DFB}}{I_S} + 1 \right) + I_{DFB} R_S \quad (1)$$

$$P_o = \eta \frac{h\nu}{e} (I_{DFB} - I_{th}) \quad (2)$$

In the above equations,  $V_J$  is the forward junction voltage,  $I_S$  is the saturation current,  $\eta$  is the quantum efficiency,  $\nu$  is the optical frequency,  $h$  the Planck constant and  $e$  the elementary charge. The modelled graphs in Fig. 3(a) are following the fitting parameters  $V_J = 58$  mV,  $I_S = 10^{-8}$  A and  $\eta = 0.06$ , whereas the experimental data accounts for the EAM pass-through and fibre coupling losses. The EML shows a forward voltage of  $\sim 1$  V at the operational bias current of 80 mA, at which a fibre-coupled power of 3 mW is obtained. A threshold current of 18 mA can be extracted from the derivative function  $dP_o/dI$ , as presented in Fig. 3(b), followed by a linear P-I relation above the threshold.

Tunability of the wavelength emission is not endeavoured but can be accomplished through tuning of the bias current  $I_{DFB}$  and the temperature  $T$ , as it will be discussed in detail in Section 5.3. Although temperature stabilization through a cooled device is not a pressing requirement, it is common that micro-Peltier elements are co-packaged with the EML chip to suit their adoption in dense wavelength division multiplexed (DWDM) grids. Such a thermo-controlled EML complies with opto-electronic packages in transistor-outline fashion [7].

EAMs work on the basis of the Franz-Keldysh and quantum-confined Stark effects [8]. By applying an electrical field, the absorption spectrum of the semiconductor is shifted, which leads to a voltage-dependent absorption of the light that passes through the EAM section. In this way, a bias-free EAM leads to just a slightly absorption of the light, while for a high negative bias voltage the signal is extinct. The absorption property

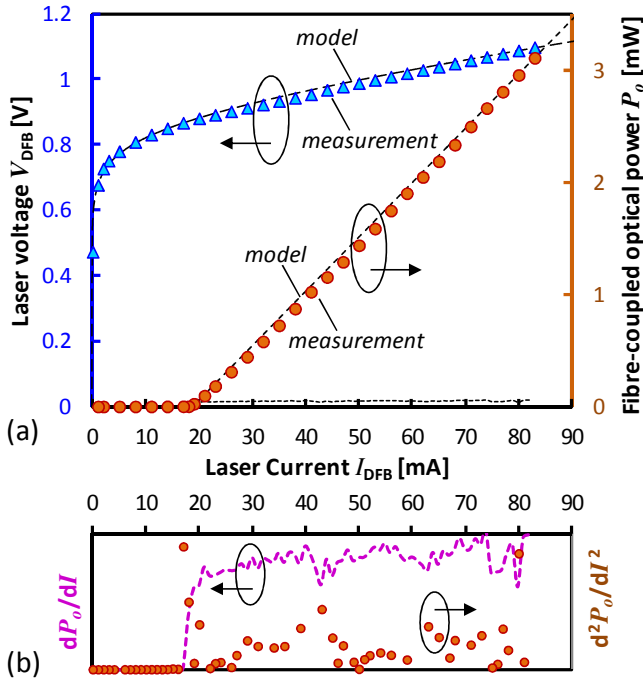


Fig. 3. VLI-characteristics of an EML.

can be used for analogue or digital high-frequency modulation of the optical output power of the EML. The non-linear transfer function  $\tau$  of the EAM follows an exponential relation to the drive  $V_{EAM}$  [9] according to

$$\tau(V_{EAM}) = a_{EAM} (1 - \varepsilon) e^{-\left(\frac{V_{EAM}}{V_a}\right)^\alpha} + \varepsilon \quad (3)$$

where  $\varepsilon$  is the minimum extinction and  $a_{EAM}$  accounts for intrinsic losses.  $V_a$  and  $\alpha$  are fitting parameters. Figure 4(a) shows this modulation function in normalized form ( $a_{EAM} = 1$ ) for  $V_a = -0.95$  V,  $\alpha = 1.4$  and  $\varepsilon = 1.3 \times 10^{-2}$ , together with normalized experimental characterization data ( $\blacklozenge$ ) of the EML at its emission wavelength of  $\lambda = 1547.82$  nm. Figure 4(b) shows that a static light extinction ( $\blacksquare$ ) of up to 9 dB can be obtained for a rather low swing of 1 V<sub>pp</sub> in terms of EAM bias voltage, at the bias point of -1.4 V. State-of-the-art work has demonstrated record values of 65 mV<sub>pp</sub> per decibel of intensity extinction ratio [10]. Moreover, large modulation bandwidths in the range of 100 GHz have been reported [11]. Together with the low driving requirements for a targeted modulation extinction ratio of 6 dB, at which an acceptable penalty of 2.2 dB applies in terms of reception sensitivity of on-off keying (OOK) [12], a high energy efficiency of 4 fJ/bit can be achieved for the radio frequency (RF) drive through EAM-based electro-optic modulation.

The sourced and modulated optical signal is then coupled to a single-mode fibre through a tapered waveguide. An anti-reflection coating at the chip facet and minimal internal optical reflections ensure stable optical emission with high purity. The EML further isolates the laser electrically from the modulator to avoid electrical crosstalk between its two active sections.

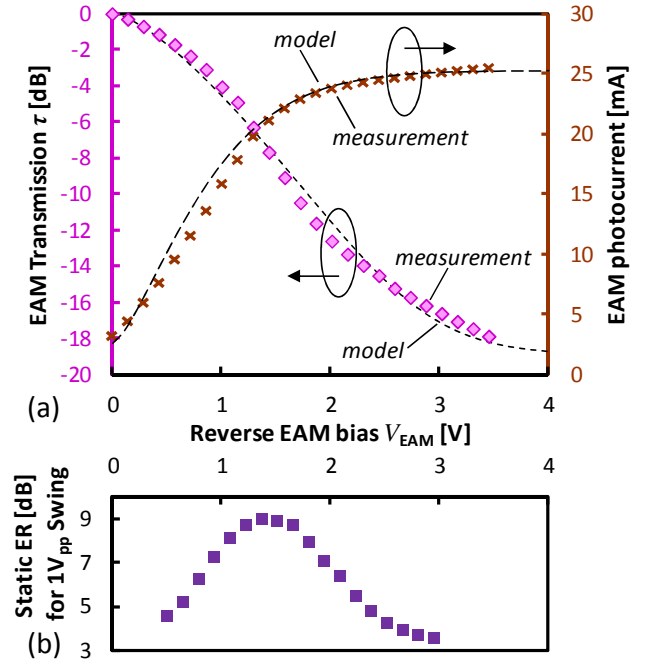


Fig. 4. Transmission and detection characteristics of an EAM.

### 3. Applications as Optical Transmitter

Although the EML represents a rather simplistic opto-electronic signal converter at first glance, there is a multitude of use cases in which it has found employment. In the following sub-sections these applications are discussed in more detail.

#### 3.1. Digital Transmission

The primary application for EMLs in datacom-centric environments has been the digital transmission at high line rates through intensity modulation and direct detection (IM/DD). EMLs have been proven to deliver high 100+ Gb/s data rates over a single wavelength using simple modulation formats, in virtue of the immense bandwidth of more than 90 GHz obtained for travelling-wave EAMs [11, 13]. OOK transmission at 100 Gb/s has been achieved with clear eye opening [11, 14]. Transmission over 10 km of standard single-mode fibre with an extinction ratio of 5 dB in absence of equalization [15] underpins the energy-effectiveness of EML technology.

As an alternative to two-level signalling, multi-level pulse-amplitude modulation (PAM) can relax the requirement on the electro-optic bandwidth, which also simplifies the opto-electronic packaging requirements. Towards this direction, demonstrations using 4-level PAM have shown equalizer-free transmission at 112 Gb/s/λ over 10 km [15]. Due to the non-linear EAM transfer function, the drive voltage for each of the quaternary PAM levels was set to a specific value through a 3-bit digital-to-analogue converter (DAC), in order to avoid uneven eye openings that would result in large reception penalties. Higher data rates beyond 200 Gb/s/λ have been achieved by employing signal equalization in the digital domain [16, 17] or probabilistic shaping in combination with 8-level PAM [18].

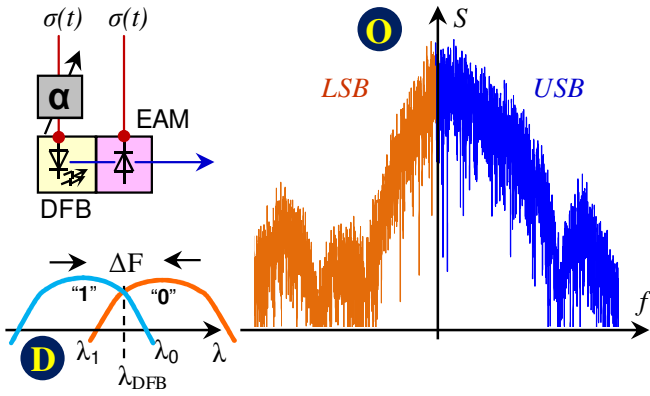


**Fig. 5.** Dual DFB and EAM modulation to spectrally sculpt the data signal.

Electrical duobinary modulation can be applied to account for a possible bandwidth limitation of packaged devices [19, 20], without resorting to power-DACs in the RF drive. Experimental demonstrations have proven this point through equalizer-free 100 Gb/s operation in combination with an RC-limited electro-optic EML bandwidth of 20 GHz [21].

Moreover, considerable effort has been put in parallel multi-lane transmitter configurations enabled through integration of WDM. Examples are 4-channel 400 Gb/s transmitters in TOSA package employing the O-band coarse WDM (CWDM) [22] or local area network WDM (LAN-WDM) [23] standards, featuring 4-PAM and 8-PAM modulation formats.

### 3.2. Spectral Sculpting

Although low-complexity integrated modulators such as the EML show a clear cost advantage compared to its bulky Mach-Zehnder modulator counterpart, data transmission over long transmission spans can quickly face dispersion limits. For example, the spectral broadening due to chirped transmission of 25-Gb/s with an EAM has been reported to impose 1-dB and 2-dB reception penalties due to chromatic dispersion after 12 and 17 km, respectively, while single-sideband transmission in virtue of simultaneous modulation of DFB and EAM sections, as discussed shortly, would extend this range to 25 and 40 km [24]. High penalties especially apply in case of high modulation extinction ratios [25] as these are accompanied by a larger spectral broadening. Additional mechanisms such as precisely tuned optical filters can address this limitation [26], and yet lead to unfavourable implications on the overall link design and an offset of the cost advantage originally gained through integrated laser-modulators.

Advantageously, the chirp property of the EAM does not impose the same dispersion limits as known for directly modulated lasers (DML); In fact, negative chirp, as it commonly applies for higher reverse EAM bias, leads to pulse compression in the anomalous dispersion regime, which can potentially offset the dispersion penalty [27]. However, in case of high data rates, even a chirp-free signal with double-sideband spectrum will quickly lead to reception penalties as the transmission reach increases. One way to address dispersive effects is to remove the redundancy in information that resides within the double-

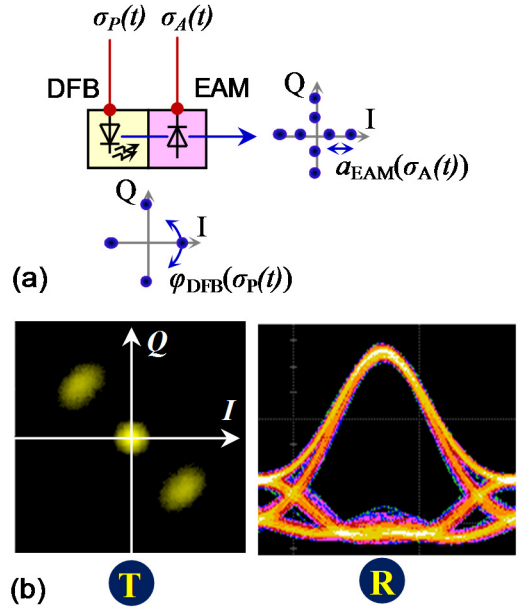


**Fig. 6.** (a) EML as vector modulator through independent DFB and EAM modulation. (b) Carved binary phase shift keying and corresponding eye diagram after demodulation.

sideband spectrum of OOK signals. This can be achieved by suppressing one of the modulation sidebands. Typically, such a single-sideband spectrum is obtained by resorting to bulky interferometric modulators that are specifically designed for this purpose [28].

The EML can serve spectral signal shaping by introducing phase correlations between consecutive bits (Fig. 5). Since it allows simultaneous and independent intensity and frequency modulation through its both sections, the latter can be used to introduce a  $\pi$ -phase shift between mark and space bits of the intensity-modulated data stream. By applying a frequency deviation  $\Delta F$  of half the data symbol rate through its DFB section (D), an equivalent  $\pi$ -phase slip is introduced at each mark bit in case that the DFB is jointly modulated with the same data stream  $\sigma(t)$  as the EAM [29]. In this way dispersive effects lead to destructive interference among two consecutive mark bits when they spread into an intermediate space bit, given that the phase of their optical carrier now alters. The dispersion tolerance can be therefore reduced, as introductorily emphasized. From a spectral point of view, the EML reduces the spectral content of a data signal to a single sideband by means of dual modulation, as it is depicted in Fig. 5 for the output spectrum (O) of the EML. The spectrum shows an unsuppressed upper modulation side band (USB) and a suppressed lower side band (LSB).

Given the polarity of the DML drive, which is sourced by the same data generator as for the EAM section, the residual intensity modulation of the DML, which typically shows an extinction ratio of  $<1$  dB, may apply in-phase or out-of-phase to the EAM modulation at larger extinction ratio [29]. The polarity of the DML drive also determines which of the modulation sidebands is suppressed.

As a prerequisite for spectral sculpting, the DFB section has to provide the same high electro-optic modulation bandwidth as the EAM does. Although dispersion tolerance can be obtained without considerably

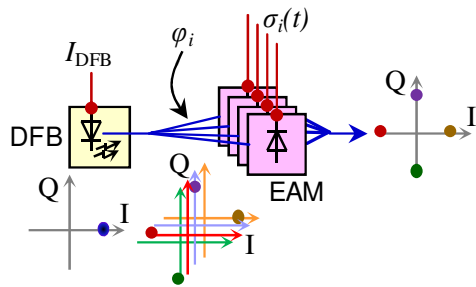


**Fig. 7.** Vector modulation through phase switching with EAM-based gates.

increasing the power consumption, complexity and cost, the laser section of the EML will be practically the limiting factor in terms of compatible modulation bandwidth. However, high electro-optic bandwidths of 24 GHz have been demonstrated for DML sections of EMLs [30]. It shall be further noted that concurrent frequency and intensity modulation exclusively performed through the DML can partially address dispersion management on its own [31]. However, independent frequency and intensity modulation is paramount in order to obtain the desired point of operation, unless strong performance trade-offs such as a reduced modulation extinction ratio are taken into consideration.

### 3.3. Complex Format Transmitter

The joint modulation of DFB laser and EAM does not necessarily have to be sourced by the same data signal. Instead, independent modulation of both EML sections can be exploited to generate complex modulation formats beyond an EML-typical link design based on an IM/DD methodology. Figure 6(a) presents such a simplified vector modulator.

Due to the chirp property of the DFB laser [32], the optical source of the EML can be regarded as phase modulator when being fed by a pre-distorted drive signal that accounts for the non-flat phase-modulation response. In order to minimize the complexity of the DFB drive  $\sigma_p$  for the purpose of chirp modulation, the phase response of the directly modulated DFB section can be therefore examined [33] and flattened through an analogue equalizer [34], which simplifies the pre-coding that is otherwise required for the direct phase modulation [35]. This method of phase-modulated signalling is also compatible with higher modulation efficiencies [36] and allows to generate, together with the EAM of the EML, quadrature amplitude modulated (QAM) formats that exploit the entire inphase/quadrature (I/Q) plane, such as 8-ary amplitude/phase shift keying [37]. No interferometric modulators are required for this purpose, which relaxes the driving and biasing requirements to obtain a stable point of operation.

Figure 6(b) presents the constellation of a 1 Gbaud return-to-zero binary phase-shift keyed signal (T) obtained through direct phase modulation of the DFB section and pulse carving through the EAM. The constellation points are clearly separated by a  $\pi$ -phase shift and a good off-pulse extinction can be noticed in the over-sampled constellation. The eye diagram after signal demodulation with an asymmetric delay interferometer (R) shows a wide eye opening. The good extinction of the space bits have been

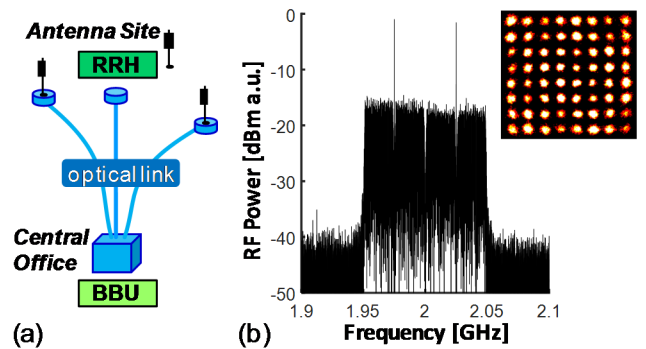


**Fig. 8.** (a) Analogue radio-over-fibre transmission for mobile fronthauling. (b) Received OFDM signal spectrum and 64-QAM constellation after analogue coherent homodyne reception with an EML.

experimentally proven to satisfy the demanding requirements for quantum key distribution [38], which evidences the quality of the complex modulation generated through the EML.

As an alternative to direct phase modulation of an EML following (multi-level drive and) an analogue or digital pre-distortion, optical phase levels can be pre-programmed and switched to the output according to the actual bit stream [39], as introduced in Fig. 7. For this purpose the continuous-wave emission of the DFB laser is split into  $N$  branches, with  $N$  being the number of constellation symbols that are to be encoded. An array of EAMs is then integrated with the DFB laser. Figure 7 shows such a switched-phase modulator for  $N = 4$ , thus yielding quadrature phase shift keying. Each of the EAM acts as a switch  $\sigma_i$  for the respective branch with fixed optical phase  $\phi_i$ . State-of-the-art work has demonstrated the feasibility of such a scheme for the generation of binary phase shift keying [39] and simultaneous two-level amplitude/phase shift keying [40].

### 3.4. Analogue Signal Transmission

Besides digital data transmission, EMLs have been adopted in analogue links where analogue signals such as they apply in wireless communication systems are to be transported between a centralized node (such as a radio baseband unit, BBU) and an end-node (such as a remote radio head, RRH), as sketched in Fig. 8(a). In such applications the analogue signal is often composed of an orthogonal frequency division multiplexed (OFDM) QAM signal, whereas the QAM sub-carriers typically feature a high modulation efficiency of 8 bits/symbol. This special case of optical signal relay demands a high linearity for its transmitting and receiving sub-systems [41], at which the analogue signal is transferred from the electrical to the optical domain, and vice versa. A high intensity extinction ratio, which equates to a high optical modulation index, will introduce a strong distortion to the electrical QAM signal that is conveyed over the intensity-modulated optical carrier. Thus, a trade-off exists between extinction ratio and launched optical power, which translates to a higher delivered power to the receiver. Earlier experimental studies reported low error vector magnitudes (EVM) of 3.7% for DML-based radio-over-fibre transmission of carrier-aggregated  $24 \times 100$  MHz 64-QAM OFDM radio-over-fibre

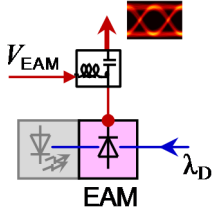


**Fig. 9.** EML as simple direct-detection receiver for an incident optical signal.

transmission [41], whereas the EML counterpart performed at a slightly increased 5.1% EVM and therefore well below the EVM limit of 8%. A stable EVM performance was obtained for radio signal transmission over a 20-km link reach in case of the EML.

It shall be stressed that broadband OFDM has also found application in digital transmission systems [42-44]. In contrast to the analogue link discussed before, OFDM is here used to equalize a non-flat end-to-end channel response of the link by means of bandwidth slicing and adaptive modulation for its sub-carriers – and thus at the expense of digital signal processing (DSP). It is therefore not bound to the strict standards of the signal to be transported over the optical layer, as it would apply in case of wireless signals for, e.g., a constant and high bit loading for the OFDM sub-carriers [45].

#### 4. The EML as Optical Receiver

As a monolithic integrated solution, EMLs effectively accomplish signal conversion from the electrical to the optical domain for the purpose of data transmission. On top of this, EMLs are able to perform signal conversion from the optical to the electrical domain in virtue of the absorption property of the EAM. This capability is not widely recognized and will be in the spotlight of the next chapters, together with potential applications. Before, the paper will discuss the direct- and coherent-detection methodology that applies to EML-based receivers.

##### 4.1. EML as Direct Photodetector

The absorption property of the EAM can be conveniently exploited for the purpose of photodetection, for which the laser section of the EML does not require to be lit (Fig. 9). Early research works have recognized the EAM as such a high-bandwidth detector [46-50]. The EAM converts the optical signal ( $\lambda_D$ ) passing through the modulator into a photocurrent, provided it is biased at absorption. Satisfactory responsivities that approach these of standard PIN photodiodes have been found.

Following the transmission function of the EAM, shown in Eq. (3), let  $\rho$  be a bias-dependent reception function according to

$$\rho(V_{EAM}) = 1 - \tau(V_{EAM}) \quad (4)$$

This function  $\rho$  is introduced, together with  $\tau$ , in Fig. 4(a) and is presented for the same EAM fitting parameters in terms of detected photocurrent. Comparison is made to the experiment ( $\times$ ), which stands in good agreement. It can be noticed that a high photocurrent, equivalent to a 1-dB

penalty of its maximum at a bias of -3.3V, is already yielded at a rather low bias of -1.37V, which renders the EAM as low-bias photodetector.

Figure 10(a) presents the received RF power at the EAM output when externally injecting an optical signal at an arbitrary wavelength  $\lambda$ , modulated by a RF tone, into the EML. The detected magnitude at the RF tone frequency is reported over a range from 1520 to 1570 nm for an EML intended at 1550 nm operation. The modelled response  $\rho$  at 1550 nm is included as dashed curve.

As it can be expected from the red-shift of the EAM absorption edge, there is no substantial change in magnitude for increasing the reverse EAM bias at short wavelengths, while long wavelengths respond to the EAM bias according to their extinction property as modulator.

The wavelength-dependent response in absorption is also evident in Fig. 10(b), which reports the swing in detected RF power for various reverse EAM biases. The maximum swing between 0 and -3.3V bias increases with  $\sim 0.39$  dB/nm. Again, a low bias for the EAM suffices the photodetection, irrespectively of the received wavelength.

Application-wise, EAMs have previously been exploited as high-bandwidth, direct-detection photodetector [46, 49] in combination with dual wavelength injection for photonic up-conversion [51] or monolithically integrated pre-amplifier sections [48], and demonstrating also optical frequency-to-amplitude demodulation functionality [52].

##### 4.2. EML as Coherent Photodetector

Despite its elementariness, the EML provides more than just a simple photodetector when being considered as receiving element. In fact, this low-cost device can be exploited for the purpose of coherent optical detection [53], as introduced in Fig. 11(a). While the EAM serves as fast in-line photodetector, similar as discussed in the previous case of direct detection, the necessary local oscillator (LO) is yielded through the DFB laser section. By tuning the DFB emission wavelength  $\lambda^*$  close to that of the incident optical data signal that is to be detected ( $\lambda_D$ ), both optical fields beat at the EAM. This leads to coherent reception for the case that the optical carrier frequencies of both, LO and data signal, are not detuned by further than the EAM bandwidth. As for traditional coherent receivers, this frequency detuning  $\delta\nu$  will determine the intermediate frequency (IF) to which the received signal is down-converted to the electrical domain.

One of the features of the EML as coherent receiver is the ability to force the detuning to  $\delta\nu = 0$ , resembling coherent homodyne detection. Unlike commonly used coherent receiver architectures, the just partially absorbing in-line EAM photodiode leads to an optical injection of the incident signal ( $\lambda_D$ ) into the DFB section. Injection locking occurs for the DFB [54], provided that the detuning  $\delta\nu$  falls within the locking range (LR), in which the DFB emission tracks the externally injected optical frequency. Figure 11(b) characterizes this frequency range under different injection power levels. Results are reported in terms of the beat frequency between an externally injected wavelength and the EML emission. In case of injection locking, this beat frequency vanishes according to  $\delta\nu = 0$ , a condition that applies for a wavelength span that depends on the level of injection. This range of locking is as wide as 9.8 GHz for an

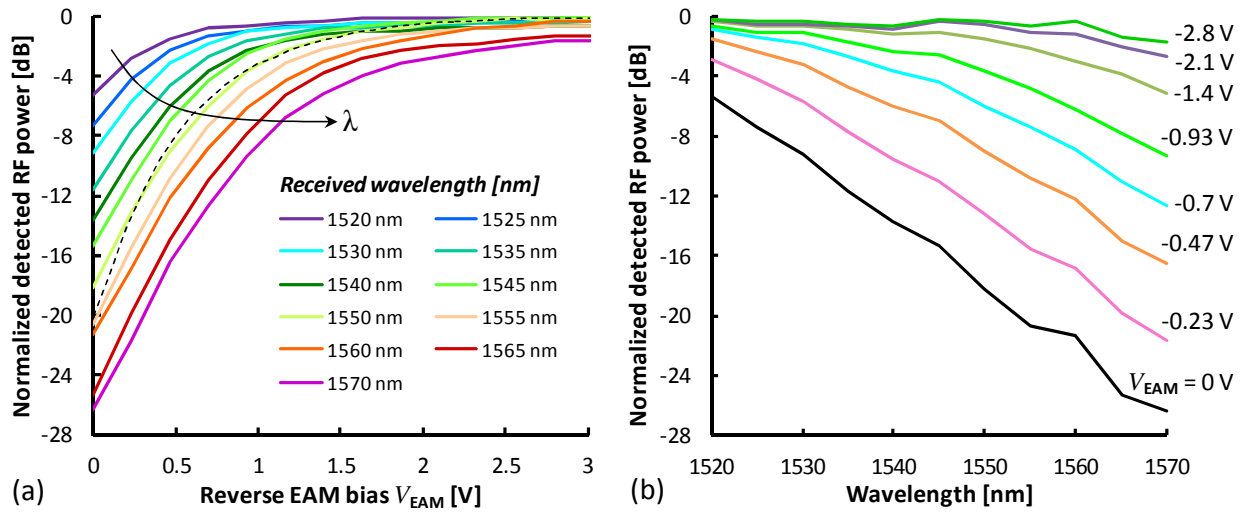


Fig. 10. Photoreception response of an EAM as function of (a) the EAM bias and (b) the wavelength.

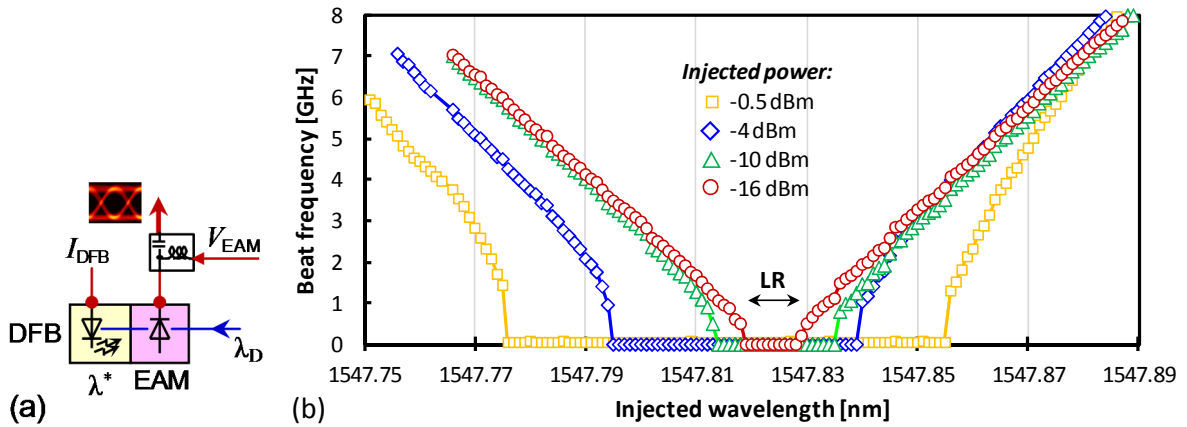


Fig. 11. (a) EML as coherent receiver. (b) Spectral range of the injection locking process as function of the received optical power.

injected power of  $-0.5$  dBm ( $\square$ ) and reduces to  $1.1$  GHz for an injection of  $-16$  dBm ( $\circ$ ). Even for a low injection power of  $-30$  dBm, a LR of more than  $200$  MHz applies. Figure 11(b) also shows an upwards detuning of the EML emission wavelength, which can be noticed by the red-shifted centres for the LR at strongest ( $\square$ ) and weakest ( $\circ$ ) injection level. It results from the frequency pushing by the injected light [55].

Tuning of the LO can be in principle facilitated through temperature and bias current control. The use of state-of-the-art temperature and bias control in combination with an EML with co-packaged micro-cooler has been shown to satisfy the requirements of having a stable optical emission frequency with a drift of less than  $90$  MHz [56], and therefore much smaller than typical values for the LR, as reported earlier. In case that the LO of the EML necessitates a wider tunability in order to access optical bandwidth beyond the thermal tuning limit, a modified DFB design [57, 58] or additional tuning mechanisms [59] can be integrated, without restricting fast LO tuning.

Polarisation-independent operation can be obtained through a polarisation diversity reception scheme [60]. In such an arrangement, for which a possible implementation is depicted in Fig. 12(a), two EMLs are fed by a polarising beam splitter (PBS) and serve as two independent coherent receivers that are each dedicated to one of the polarization

tributaries. A polarization-independent electrical reception signal is yielded by summing the outputs of the two tributaries. This operation was experimentally assessed over a field-installed fibre link. The received polarisation, which results from the transform along the link, is shown on the Poincare sphere for the entire measurement duration of  $\sim 200$  minutes. As Fig. 12(b) highlights, the received constellation of an 8-QAM broadband OFDM sub-carrier remains without fading penalty in presence of the polarization transform. Strong power fading induced by polarization-selective extinction in one of the branches may require to blank the respective received signal [60] in case that a high dynamic optical power range is endeavoured, which would eventually cause an unlocked LO.

The technologically lean realization of coherent homodyne detection is a remarkable result: There is no frequency difference between the LO and the received data signal, which greatly simplifies the signal processing at the electrical domain. In fact, experimental demonstrations [61, 62] were able to fully omit any means of analogue or digital signal processing for transparent signal detection, rendering the EML-based coherent receiver as an implementation with a high degree of conceptual simplicity. It shall be stressed that the case of homodyne detection is common for wireless receivers, where synthesizers can be realized with high

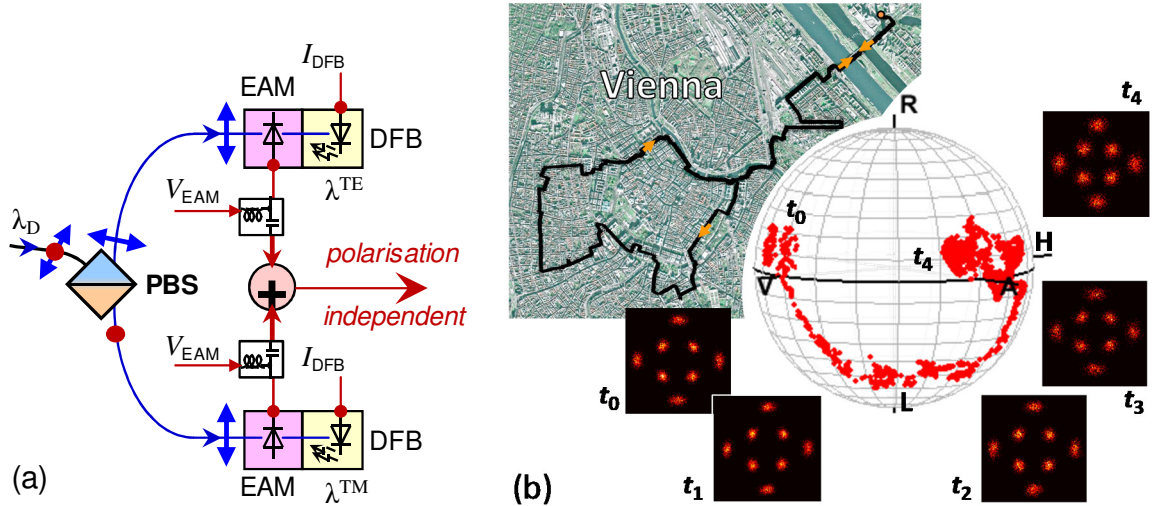


**Fig. 12.** (a) Polarisation-independent EML-based coherent receiver. (b) Long-term measurement over field-installed fibre link.

accuracy. Nonetheless, a synchronization of optical sources is by no means straight-forward. The EML-based coherent receiver builds on a fast and all-optical phenomenon and obviates the need for fast or complex opto-electronic phase-locked loops [63, 64] to support this challenging process.

## 5. Applications as Optical Receiver

The conceptual simplicity of the EML-based coherent receiver has prompted explorations into applications that require cost-effective detection schemes. The following sub-sections highlight a few use cases that benefit from the specifics inherent to the coherent reception methodology of the EML.

### 5.1. Coherent Analogue Radio-over-Fibre Transmission

The emergence of the fifth generation (5G) of wireless communications has sparked cloud-based radio access. As introduced previously in Section 3.4, computational resources responsible for the signal processing in such a cloud-enabled network are pooled in BBUs at a centralized datacenter, while the field-deployed RRHs are implemented with the lowest possible complexity [65]. Since the distance between RRHs and BBU can reach up to 20 km while still satisfying the strict latency requirements, optical fronthauling has been identified as one solution for signal relay between the two end-points [66]. However, it is paramount to preserve the signal integrity when translating the radio signal from the electrical to the optical domain, and vice versa. Although analogue optical signal transmission would be of great interest due to its simplified optical transceivers [67, 68], the non-linearity of opto-electronic conversion often calls for digitized radio signal transmission [69, 70].

Moreover, coherent reception can contribute through its sensitivity gain and access to ultra-dense multiplexing in the wavelength domain [71]. Under the umbrella of analogue radio signal transmission, homodyne reception is the methodology of choice, in order to retain a simplified transceiver scheme that does not resort to DSP functions for the purpose of signal recovery. Towards this direction, the coherent homodyne EML receiver can be beneficial, as

proven in earlier experiments [61]. It has been shown that the RF carrier frequency of the optically transmitted radio signal is perfectly resembled after optical signal detection, in virtue of wavelength locking between LO and transmitted signal. Figure 8(b) presents an example for an OFDM radio signal, transmitted at a RF carrier frequency of 2 GHz, after homodyne detection with an EML, and the corresponding signal constellation for its 64-QAM sub-carriers. The RF carrier frequency is preserved and the OFDM boundaries and pilot tones are not washed out. This confirms correct homodyne detection. Moreover, a clear constellation is obtained. Real-time end-to-end performance evaluation with a software-defined radio unit have confirmed the signal integrity by means of error counting, for which block error ratios below  $10^{-4}$  have been obtained. This evidences the transparency of the coherent analogue optical fronthaul link, which is able to omit analogue-to-digital conversion (ADC/DAC) technology for the purpose of digitized optical radio signal transmission.

It shall be stressed that for case of an unbiased DFB laser, meaning to perform direct-detection with the EML, no data signal was discernible above the noise floor. This evidences the sensitivity gain obtained through the coherent detection methodology.

If the LO and the incident data signal intentionally feature a large detuning, yet within the opto-electronic reception bandwidth of the EAM and thus corresponding to the case of coherent heterodyne detection, the data signal can be up-converted [72]. The photonic up-conversion of wireless signals can greatly ease the generation of millimetre-wave radio signals.

### 5.2. Coherent Reception at the Packet Level

Many applications of optical communications build on network architectures that go beyond simple point-to-point links. In these any-to-any architectures, many transmitters may communicate with a single receiver, or vice versa. This implies that signals originate from different optical sources at  $\nu^{(i)}$ , and yet shall be received through a time-shared optical receiver operating in a time division multiple access (TDMA) mode. In such a scenario, sketched in Fig. 13(a), the receiver needs to swiftly adapt to the

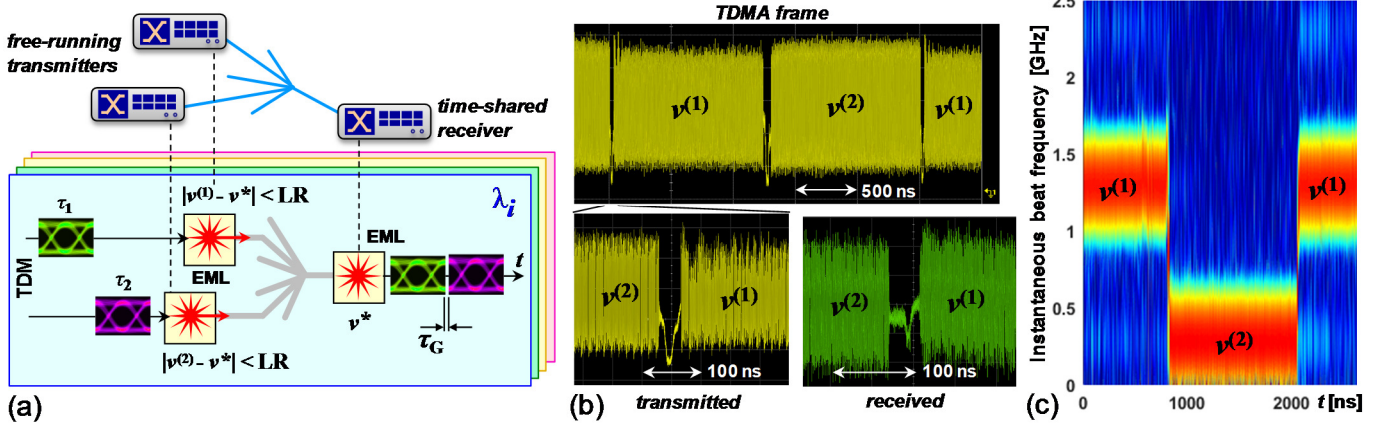


**Fig. 13.** (a) Reception in TDMA mode. (b) Delivered and received TDMA frame. (c) Instantaneous frequency shift of the LO of the EML-based receiver for dual packet injection.

incident data burst at  $\tau_i$ , ideally without employing an extra training signal. This becomes a fairly complex exercise when considering coherent optical reception, for which fast frequency offset and carrier phase recovery are to be sequentially applied to the incident optical packets [73].

In case of the EML-based receiver, the fast all-optical locking process of the DFB laser can assist the required synchronization process. First, the emission of several free-running transmitters at  $\nu^{(i)}$  occurs in the spectral proximity of the receiver ( $\nu^*$ ). It particularly falls within its locking range so that homodyne reception can be established for all incident data bursts. Second, the locking response is fast [74]. As it has been investigated in a recent work, the dynamic locking process for TDM reception supports small inter-packet gaps in the order of 10 to 100 ns [56]. Figure 13(b) shows an optically delivered TDMA frame consisting of two data packets and the received frame after coherent optical detection through an EML. The corresponding locking response of the LO of the EML receiver has been characterized through beating the EML emission with a stable reference laser. Figure 13(c) presents the frequency shift in beat frequency as the EML receives burst data at the optical frequencies  $\nu^{(1)}$  and  $\nu^{(2)}$ . The two burst envelopes are accompanied by two instantaneous frequency deviations of 450 and -570 MHz from the beat note of the unlocked LO ( $\nu^*$ ) at 850 MHz. Fast locking can be obtained, which enables a short guard interval  $\tau_G$  of only 40 ns between the data bursts [56].

The compatibility with TDMA schemes and coherent reception enables to collapse a high number of ultra-dense WDM sub-wavelengths over a filterless, high-split distribution network, as it is of interest in short-reach architectures in the fields of optical access and intra-datacentre networks. Moreover, the fast locking of the EML-based receiver supports short-lived data flows as they apply in datacentre environments.

### 5.3. Spectral Monitor

The tuning of the EMLs emission frequency  $\nu^*$  can be in the simplest case made through either current  $I_{\text{DFB}}$  [75] or temperature  $T$  [76] control. Characterization data for the spectral tuning is presented in Fig. 14, which shows the tuning efficiency in the DFB laser emission for a variation in DFB bias current and temperature, respectively, as

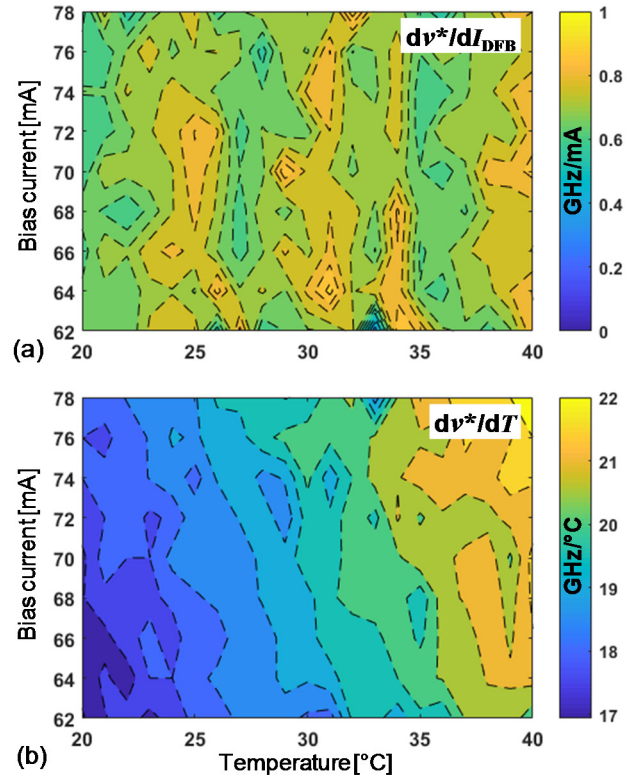


**Fig. 14.** Tuning efficiency of the EML emission frequency through (a) DFB bias current and (b) temperature.

function of the  $T/I_{\text{DFB}}$  operation point. Current-induced tuning allows for fine tuning at  $\sim 0.75$  GHz/mA. Coarse alignment of the EML emission wavelength over more than 300 GHz is conducted through temperature tuning, with an efficiency of 18 to 21 GHz/ $^{\circ}\text{C}$ .

Continuous tuning of the LO emission frequency of the EML receiver enables to down-convert an optical slice of the received input within the optical tuning range to the electrical domain. The RF power within an electrically defined resolution bandwidth can then be integrated in order to obtain an opto-electronic RF spectrum analyser [77]. Figure 15(a) shows such an analyser, which yields an RF output that is proportional to the optical power  $P_{\text{opt}}$  incident to the EML, as function of the EML's actual emission frequency  $\nu^*$  and the corresponding deviation  $\Delta\nu^*$  that results from the detuned bias point. The down-converted

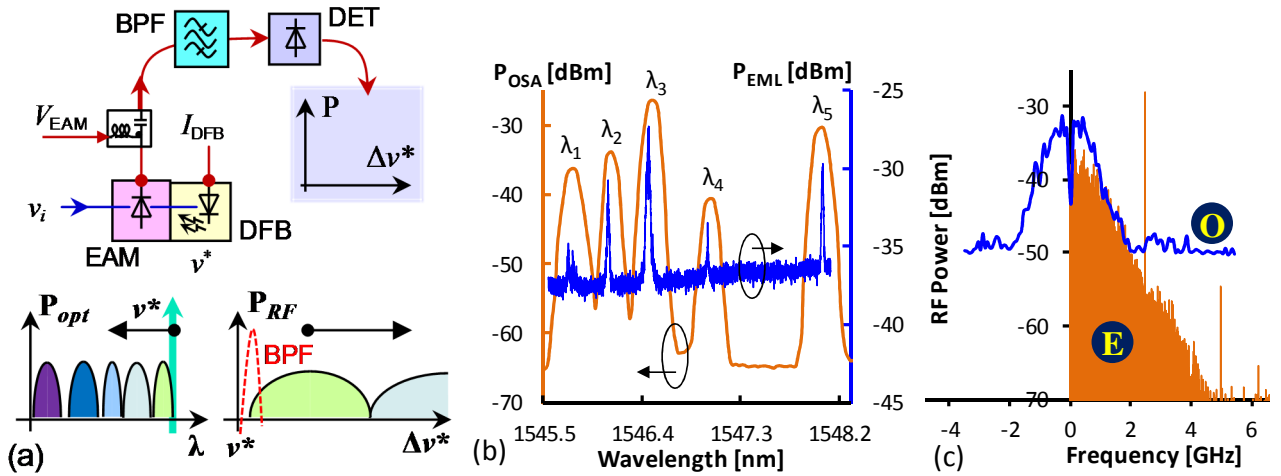


**Fig. 15.** (a) EML as opto-electronic RF spectrum analyzer. (b) Comparison between spectra acquired through an optical spectrum analyser with a resolution bandwidth of 0.1 nm and the EML-based spectrum analyser. (c) Resolved signal spectrum for opto-electronic EML-based analyser (O) and electrical RF spectrum analyser (E).

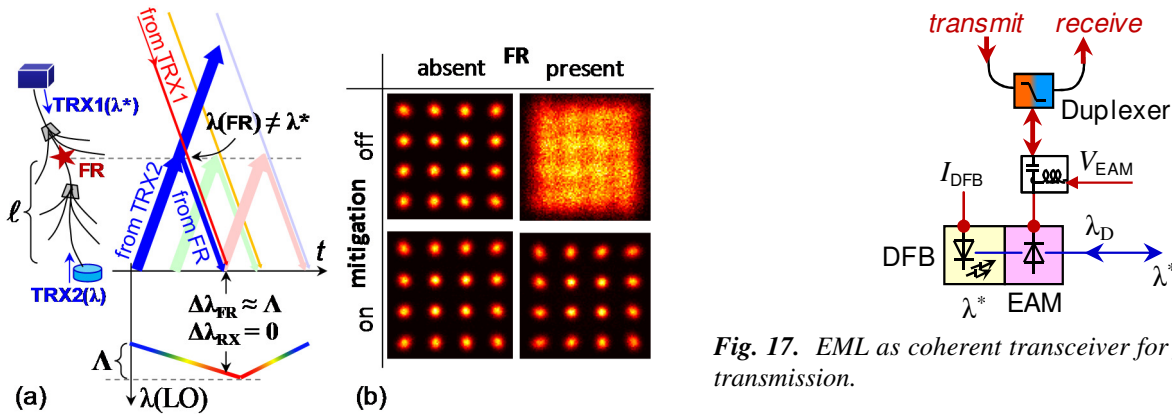


**Fig. 16.** (a) Spectrally floating transmission with continuously detuned optical emission frequency. (b) Mitigation of reflection crosstalk of a FR present in the fiber plant through synchronized detuning from its induced crosstalk.

electrical signal is filtered by a narrow RF bandpass filter (BPF) that defines the resolution bandwidth, and subsequently integrated through a RF detector (DET). This yields a signal that is directly related to the optical power received at the actual frequency setting  $\Delta\nu^*$ .

Figure 15(b) shows an example of such a spectral sweep, which covers the input signals from  $\lambda_1$  to  $\lambda_5$ . The acquired spectrum  $P_{EML}$  of the EML-based monitor agrees well to that obtained through an optical spectrum analyser ( $P_{OSA}$ ) with a resolution bandwidth of 0.1 nm. The absolute error in centre wavelength varies from -36 to +5 pm, while the error in magnitude reaches from -4.6 to +4.5 dB. Given the much narrower resolution bandwidth for spectral analysis in the RF domain, the EML-based monitor enables a higher resolution, fine enough to resolve the modulation spectrum. This is demonstrated in Fig. 15(c), showing a 2.5 Gb/s OOK signal acquired through the EML-based spectrum analyser (O) in comparison to the electrically resolved spectrum of the sourced data signal as obtained through an RF spectrum analyser (E).

**Fig. 17.** EML as coherent transceiver for full-duplex data transmission.

The re-use of state-of-the-art transmitter technology such as an EML as continuously-tuned, coherent monitor enables to distributively deploy monitoring functionality network-wide.

#### 5.4. Spectrally Floating Transmission

The locking of an EML-based coherent receiver does not have to build on an optical signal with static wavelength assignment. Homodyne reception applies as long as the received emission and the LO feature approximately the same optical frequency, which nevertheless can be a function of time [78]. In this way, data transmission is not bound to a certain wavelength but “floats” within the optical spectrum that is accessible through the EML.

There are several advantages that such a spectrally floating transmission offers. By applying a frequency hopping scheme in the optical domain, inherent security is provided since only transmitting and receiving party know the hopping sequence through which data transmission is possible. Moreover, migrating from a static to a dynamic wavelength assignment makes the data transmission robust against crosstalk that would jam a certain channel. Figure 16(a) presents such a scenario in which two transceivers (TRX) apply and synchronize a sweep in their emission wavelengths so that it deviates by  $\Lambda$  at its maximal excursion. This sweep, which does not prevent data transmission, enables the mitigation of crosstalk that arises

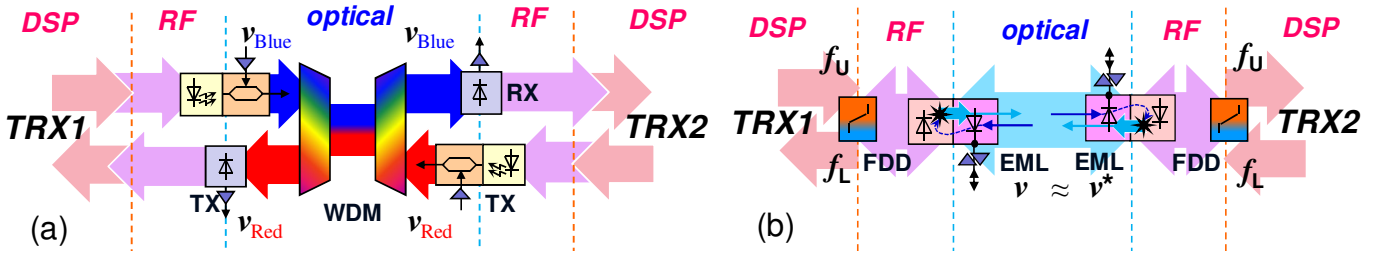


**Fig. 18.** Signal chain for the optical link in case of (a) traditional bidirectional link with down- and upstream transmission in different wavebands, and (b) bidirectional link with full-duplex, EML transceivers.

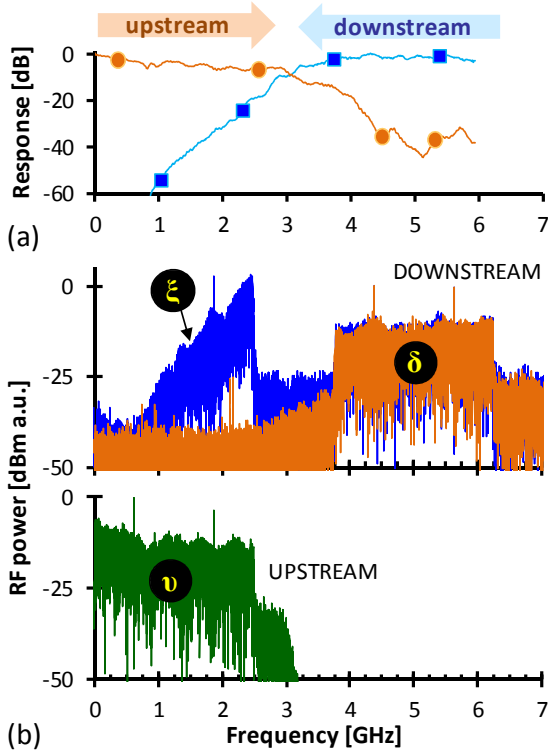


**Fig. 19.** (a) Frequency sub-bands for FDD operation and (b) corresponding signal spectra obtained at the down- and upstream branches of the EML-based transceiver.

at impairments in the fibre plant, such as a Fresnel reflection (FR). The sweep sequence is tailored to maximize the deviation in wavelength between the emitted signal and the FR crosstalk,  $\Delta\lambda_{FR}$ , to the swing  $\Lambda$ , while the deviation between transmitter and receiver,  $\Delta\lambda_{RX}$ , remains zero due to a synchronized sweep at both end-points.

Figure 16(b) shows the received OFDM signal constellation for data transmission that involves such a reflection in the lightpath [78]. For static wavelength assignment, the constellation is strongly blurred when the FR is present due to its induced crosstalk, for which results are shown for an optical signal-to-reflection ratio of 1 dB. This prevents any data from being received. When the light emission at the transmitter and the LO are jointly swept and synchronized to each other, the detrimental impact of the FR can be mitigated, provided that the detuning sequence is adjusted to the reach  $\ell$  of the FR. For the presented case, the FR was situated at a reach of  $\ell = 4.3$  km and the sawtooth frequency used as sweep sequence was 12.1 kHz. The induced reception penalty can then be reduced by 93%,

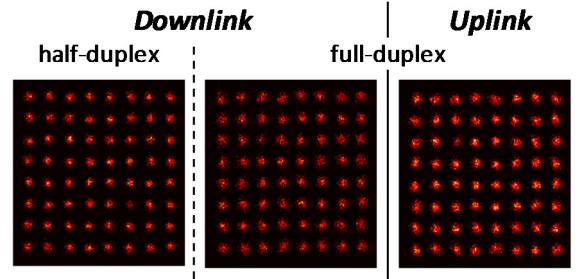


**Fig. 20.** Received constellations after coherent homodyne radio-over-fibre transmission for half- and full-duplex mode of operation at the EML-based downlink receiver.

which is evidenced by the clear constellation. This proves correct coherent homodyne reception with the EML receiver under a dynamic allocation for the channel wavelength.

## 6. The EML as Coherent Transceiver

Being able to transmit and receive in virtue of the dual-function EAM element, the EML can simultaneously perform both tasks of converting a signal from the electrical to the optical domain and vice versa [79]. Remarkably, this transceiver function, sketched in Fig. 17, can be realized in full-duplex operation rather than dedicating a TDM sub-frame for transmission and coherent reception, as it would apply for a half-duplex transceivers.

A characteristic of the EML as full-duplex transceiver is the point at which it applies its directional split in the signal chain. Figure 18(a) presents a traditional link with two transceivers that exploit WDM to separate down- and upstream direction. Given the maturity of waveband splitters, this ensures negligible crosstalk between the directional communication sub-channels. However, the component count is doubled in order to obtain full-duplex transmission. In case of the EML-based transceiver, which is employed in the full-duplex link shown in Fig. 18(b), the transceiver simplifies and now features only a single bidirectional element with single fibre access and a single RF port per polarization. The directional split between down- and upstream is now implemented in the electrical rather than the optical domain. To do so, a suitable electrical duplexing methodology is to be employed.

Since the EAM typically features a large electro-optic bandwidth, frequency division duplexing (FDD) becomes an attractive option. The duplexer slices the EAM bandwidth into two frequency bands  $f_U$  and  $f_L$ , dedicated to each of the transmission directions.

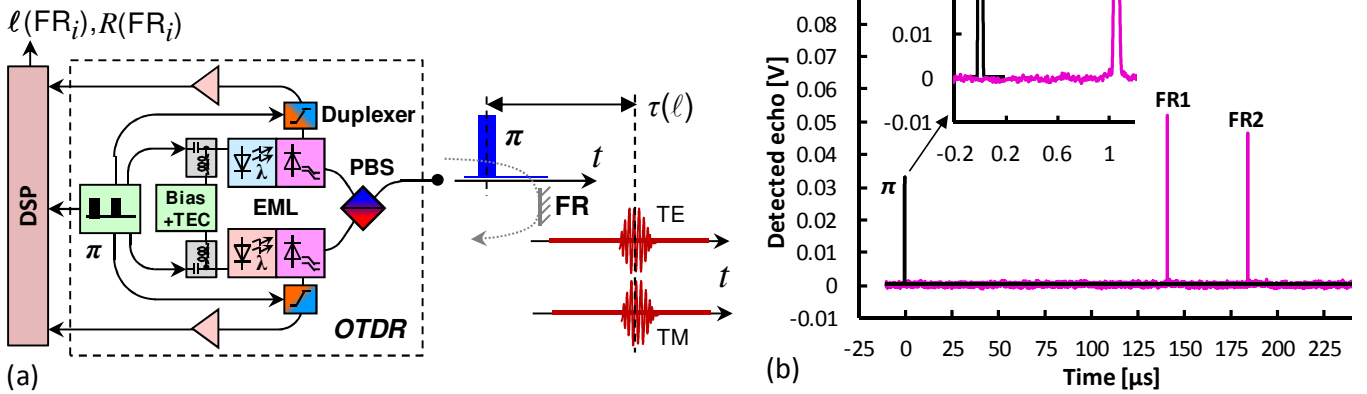


**Fig. 21.** (a) Polarisation-independent OTDR based on dual-EML transceiver. (b) Obtained echo signatures arising at three FRs along a fibre link.

### 6.1. Full-Duplex Digital and Analogue Signal Transmission

Figure 19(a) shows an example for FDD [79] with frequency bands for downstream (■) and upstream (●) selected according to 2.5 Gbaud OFDM transmission. The signal spectra can be separated with good rejection, which is evidenced in Fig. 19(b) by the rather weak crosstalk ( $\xi$ ) of the strong upstream launch that is seen in the received downstream signal spectrum ( $\delta$ ) when full-duplex transmission is performed with a single EML-based coherent transceiver. The downstream penalty due to full-duplex transmission corresponded to a 10% drop in delivered OFDM data rate. This penalty trades well with the greatly reduced complexity for the transceiver. The simultaneous transmission of data through the EAM did not negatively impact the coherent homodyne reception and, in particular, the injection locking process.

The full-duplex transmission performance has been further investigated in the context of analogue radio-over-fibre transmission [80]. The down- and uplink RF carrier frequencies were 2 and 5.2 GHz, respectively, thus adhering to the FDD scheme. Excellent signal integrity has been obtained for the penalty-sensitive radio signal. The EVM penalty due to full-duplex transmission of a 64-QAM OFDM radio signal was as low as 0.7% for the radio downlink when activating the much stronger radio uplink drive connected to the downlink receiver through the FDD duplexer. The corresponding downlink constellation diagrams for absent and present radio uplink are presented in Fig. 20.

The aforementioned performances for full-duplex transmission have been obtained using a single EML-based transceiver at the tail-end of the optical communication link. This corresponds to a scenario where the tail-end equipment is in focus of a complexity reduction, as it is paramount for telecom segments with cost-sensitive end-user systems, such as optical access networks. However, it is possible to have a link configuration with low complexity at both, head- and tail-end, as it is actually introduced in Fig. 18(b). Face-to-face EML configurations as full-duplex transceiver at either link end have been recently demonstrated [81]. Long-term EVM measurements have confirmed the stable radio signal

transmission over such an EML-to-EML arrangement, for which sporadic rather than excessive EVM excursions have been observed.

### 6.2. Optical Ranging

Besides applications in data transmission, an EML-based transceiver can serve fibre plant monitoring through concurrent probing and signal reception as required for optical time domain reflectometry (OTDR). Figure 21(a) presents an example for such an EML-based OTDR system. The EAM is switched between transparency for pulse probe ( $\pi$ ) emission and absorption for coherent heterodyne detection of the echo that arises at the fibre plant. A dual-EML architecture with detuned LOs enables polarisation-insensitive operation, for which the pulse probe is additionally frequency modulated to account for the worst-case polarization of the incident echo [82]. Figure 21(b) shows the acquired echo after envelope detection of the received reflection signature for a fibre-optical link with three partially attenuated Fresnel reflections at 104 m, 14.3 km and 18.6 km. After a 2-ms short time-of-arrival measurement and reflection ranging, the magnitude and reach can be precisely obtained for each of the reflections, leaving error values of less than 3% and 9% for reach and reflectance, respectively. Optical return loss values of up to 42.5 dB are compatible with the EML-based OTDR [82]. These experimental results prove that transmitter technology can accommodate field-distributed monitoring functionality, characterized by short acquisition times.

## 7. Conclusion

This paper has reviewed the state-of-the-art in EML technology as optical transmitter, receiver and full-duplex transceiver. The ability to effectively convert signals from the electrical to the optical domain with low driving requirements of down to 60 mV<sub>pp</sub> per dB of extinction ratio and the offering of high modulation bandwidths in the range of 100 GHz have rendered the EML as an attractive candidate for a technical strategy that can significantly reduce both, capital and operating expenditures in short-reach networks. Parallel links with multiple lanes, multi-level formats and suitable space division multiplexing

schemes can accommodate Tb/s data rates through use of commodity opto-electronics, without the need for equalization or DSP functions.

Moreover, recent research work has proposed the dual-function of the EML as an optical receiver. The disruptive concept of coherent homodyne detection with an all-optically locked LO and its compatibility with full-duplex data transmission through simultaneous use of the EAM as modulator and photodetector has opened new vistas, especially for cost-sensitive applications. Towards this direction, full-duplex coherent analogue radio signal transmission has been shown to benefit from the preservation of the signal integrity of 64-QAM OFDM formats. Low full-duplex implementation penalties have pointed towards an unexplored potential of legacy EML technology, which for long time had been mostly recognised for transmitter applications.

Although the traditional EML setting with a single DFB and a single EAM may limit the practical applicability of the demonstrated concepts, modern photonic integration technology is undoubtedly providing a fruitful ground that supports the take-up of novel transceiver schemes. By doing so, it will enable flexible, tunable and multi-functional opto-electronics that combine high bandwidth, energy efficiency, advanced modulation and coherent reception in novel transceiver layouts, to eventually initiate the next cycle of the digital evolution.

## 8. Acknowledgments

The author would like to thank Dinka Milovančev, Nemanja Vokić and Fotini Karinou for the fruitful discussions.

This work was supported in part by the European Research Council (ERC) under the European Union's Horizon 2020 research and innovation programme (grant agreement No 804769).

## 9. References

- [1] Winzer, P.J., Neilson, D.T.: 'From Scaling Disparities to Integrated Parallelism: A Decathlon for a Decade', *IEEE J. Lightwave Technol.*, 2017, 35, (5), pp. 1099-1115
- [2] Singh, A., Ong, J., Agarwal, A., et al.: 'Jupiter Rising: A Decade of Clos Topologies and Centralized Control in Google's Datacenter Network', *Proc. ACM Special Interest Group on Data Communication*, London, United Kingdom, Aug. 2015, pp. 183-197
- [3] Essiambre, R.J., Kramer, G., Winzer, P.J., et al.: 'Capacity Limits of Optical Fiber Networks', *IEEE J. Lightwave Technol.*, 2010, 28, (4), pp. 662-701
- [4] Duncanson, J.: 'Inverse multiplexing', *IEEE Comm. Mag.*, 1994, 32, (4), pp. 34-41
- [5] Wakita, K., Kotaka, I., Asai, H., et al.: 'High-speed and low-drive voltage monolithic multiple quantum-well modulator/DFB laser light source', *IEEE Photon. Technol. Lett.*, 1992, 4, pp. 16-18
- [6] Doerr, C.: 'Monolithic InP Photonic Integrated Circuits for Transmitting or Receiving Information with Augmented Fidelity or Spectral Efficiency'. in: Nakazawa, M., Kikuchi, K., Miyazaki, T. (Eds.): 'High Spectral Density Optical Communication Technologies' (Springer, 2010).
- [7] Han, Y.T., Kwon, O.K., Lee, D.H., et al.: 'A cost-effective 25-Gb/s EML TOSA using all-in-one FPCB wiring and metal optical bench', *OSA Opt. Expr.*, 2013, 21, (22), pp. 26962-26971
- [8] Li, G.L., Yu, P.K.L.: 'Optical Intensity Modulators for Digital and Analog Applications', *IEEE J. Lightwave Technol.*, 2003, 21, (9), pp. 2010-2030
- [9] Salvatore, R.A., Sahara, R.T., Bock, M.A., et al.: 'Electroabsorption Modulated Laser for Long Transmission Spans', *IEEE J. Quantum Electron.*, 2002, 38, (5), pp. 464-476
- [10] Dalir, H., Takahashi, Y., Koyama, F.: 'Compact low driving voltage (<400 mVpp) electro-absorption modulator laterally integrated with VCSEL', *IEE Electron. Lett.*, 2014, 50, (2), pp. 101-103
- [11] Ozolins, O., Pang, X., Iglesias Olmedo, M., et al.: '100 GHz Externally Modulated Laser for Optical Interconnects' *IEEE J. Lightwave Technol.*, 2017, 35, (6), pp. 1174-1179
- [12] Schrenk, B., Bakopoulos, P., Kehayas, E., et al.: 'All-Optical Carrier Recovery Scheme for Access Networks with Simple ASK Modulation', *IEEE/OSA J. Opt. Comm. and Netw.*, 2011, 3, pp. 704-712
- [13] Lewen, R., Irmscher, S., Westergren, U., et al.: 'Segmented Transmission-Line Electroabsorption Modulators', *IEEE J. Lightwave Technol.*, 2004, 22, (1), pp.172-179
- [14] Kazmierski, C., Konczykowska, A., Jorge, F., et al.: '100 Gb/s Operation of an AlGaInAs Semi-Insulating Buried Heterojunction EML' *Proc. Opt. Fiber Comm. Conf., San Diego, United States, Mar. 2009, OThT7*
- [15] Kanazawa, S., Fujisawa, T., Takahata, K., et al.: 'Flip-Chip Interconnection Lumped-Electrode EADFB Laser for 100-Gb/s/λ Transmitter', *IEEE Photon. Technol. Lett.*, 2015, 27, (16), pp. 1699-1701
- [16] Kanazawa, S., Yamazaki, H., Nakanishi, Y., et al.: '214-Gb/s 4-PAM Operation of Flip-Chip Interconnection EADFB Laser Module', *IEEE J. Lightwave Technol.*, 2017, 35, (3), pp. 418-422
- [17] Pang, X., Ozolins, O., Lin, R., et al.: '200 Gbps/Lane IM/DD Technologies for Short Reach Optical Interconnects', *IEEE J. Lightwave Technol.*, 2020, 38, (2), pp. 492-503
- [18] Zhang, J., Yu, J., Zhao, L., et al.: 'Demonstration of 260-Gb/s Single-Lane EML-Based PS-PAM-8 IM/DD for Datacenter Interconnects', *Proc. Opt. Fiber Comm. Conf., San Diego, United States, Mar. 2019, W4I.4.*

- [19] Price, A.J., Le Mercier, N.: 'Reduced bandwidth optical digital intensity modulation with improved chromatic dispersion tolerance', *IEEE Electron. Lett.*, 1995, 31, (1), pp. 58-59
- [20] Verplaetse, M., Lin, R., Van Kerrebrouck, J., et al.: 'Real-Time 100 Gb/s Transmission Using Three-Level Electrical Duobinary Modulation for Short-Reach Optical Interconnects', *IEEE J. Lightwave Technol.*, 2017, 35, (7), pp. 1313-1319
- [21] Abbasi, A., Verbist, J., Shiramin, L.A., et al.: '100-Gb/s Electro-Absorptive Duobinary Modulation of an InP-on-Si DFB Laser', *IEEE Photon. Technol. Lett.*, 2018, 30, (12), pp. 1095-1098
- [22] El-Fiky, E., Osman, M., Samani, A. et al.: 'First demonstration of a 400 Gb/s 4 $\lambda$  CWDM TOSA for datacenter optical interconnects', *OSA Opt. Expr.*, 2018, 26, (16), pp. 19742-19749
- [23] Kawamoto, Y., Ohata, N., Murao, T., et al.: 'An integrated LAN-WDM 400-Gb/s (53Gbaud-PAM4) EML TOSA', *Proc. Optoelectr. Comm. Conf. / Photon. Switching and Comp. Conf.*, Fukuoka, Japan, Jul. 2019, WD1-3
- [24] Anfray, T., Aupetit-Berthelemot, C., Kechaou, K., et al.: 'Simulation of SSB-LC with D-EML for extended PON beyond the Chromatic Dispersion Limit', *IEEE J. Lightwave Technol.*, 2012, 30, (19), pp. 3089-3095
- [25] Corvini, P.J., Koch, T.L.: 'Computer Simulation of High-Bit-Rate Optical Fiber Transmission Using Single-Frequency Lasers', *IEEE J. Lightwave Technol.*, 1987, 5, (11), pp. 1591-1595
- [26] Mahgerefteh, D., Matsui, Y., Zheng, X., et al.: 'Applications of 40-Gb/s Chirp-Managed Laser in Access and Metro Networks', *IEEE J. Lightwave Technol.*, 2009, 27, (3), pp. 253-265
- [27] Park, Y.K., Nguyen, T.V., Morton, P.A., et al.: 'Dispersion-Penalty-Free Transmission Over 130-km Standard Fiber Using a 1.55- $\mu$ m, 10-Gb/s Integrated EA/DFB Laser with Low-Extinction Ratio and Negative Chirp', *IEEE Photon. Technol. Lett.*, 1996, 8, (9), pp. 1255-1257
- [28] Fonseca, D., Cartaxo, A.V.T., Monteiro, P.: 'Optical Single-Sideband Transmitter for Various Electrical Signaling Formats', *IEEE J. Lightwave Technol.*, 2006, 24, (5), pp. 2059-2069
- [29] Kim, H., Kim, S.K., Lee, H., et al.: 'A novel way to improve the dispersion-limited transmission distance of electroabsorption modulated lasers', *IEEE Photon. Technol. Lett.*, 2006, 18, (8), pp. 947-949
- [30] Kim, H.: 'EML-Based Optical Single Sideband Transmitter', *IEEE Photon. Technol. Lett.*, 2008, 20, (4), pp. 243-245
- [31] Binder, J., Kohn, U.: '10 Gbits/s-dispersion optimized transmission at 1.55  $\mu$ m wavelength on standard single mode fiber', *IEEE Photon. Technol. Lett.*, 1995, 6, (4), pp. 558-560
- [32] Bjerkan, L., Royset, A., Hafskjaer, L., et al.: 'Measurement of Laser Parameters for Simulation of High-speed Fiberoptic Systems', *IEEE J. Lightwave Technol.*, 1996, 14, (5), pp. 839-850
- [33] Sato, K., Kuwahara, S., Miyamoto, Y.: 'Chirp Characteristics of 40-Gb/s Directly Modulated Distributed-Feedback Laser Diodes', *IEEE J. Lightwave Technol.*, 2005, 23, (11), pp. 3790-3797
- [34] Cano, I.N., Lerin, A., Polo, V., et al.: 'Direct Phase Modulation DFBs for Cost-Effective ONU Transmitter in udWDM PONs', *IEEE Photon. Technol. Lett.*, 2014, 26, (10), pp. 973-975
- [35] Vodhanel, R.S.: '5 Gbit/s Direct Optical DPSK Modulation of a 1530-nm DFB Laser', *IEEE Photon. Technol. Lett.*, 1989, 1, (8), pp. 218-220
- [36] Cano, I.N., Lerin, A., Prat, J.: 'DQPSK Directly Phase Modulated DFB for Flexible Coherent UDWDM-PONs', *IEEE Photon. Technol. Lett.*, 2016, 28, (1), pp. 35-38
- [37] Velásquez, J.C., Tabares, J., Prat, J.: 'Differential 8-APSK monolithically integrated dual-EML transmitter for flexible coherent PONs', *OSA Opt. Lett.*, 2019, 44, (11), pp. 2760-2763
- [38] Schrenk, B., Hentschel, M., Hübel, H.: 'Single-Laser Differential Phase Shift Transmitter for Small Form-Factor Quantum Key Distribution Optics', *Proc. Opt. Fiber Comm. Conf.*, San Diego, United States, Mar. 2018, Th3E.3
- [39] Kazmierski, C., Carrara, D., Lawniczuk, K., et al.: '12.5GB Operation of a Novel Monolithic 1.55 $\mu$ m BPSK Source Based on Prefixed Optical Phase Switching', *Proc. Opt. Fiber Comm. Conf.*, Anaheim, United States, Mar. 2013, OW4J.8.
- [40] de Valicourt, G., Mardoyan, H., Mestre, M.A., et al.: 'Monolithic Integrated InP Transmitters Using Switching of Prefixed Optical Phases', *IEEE J. Lightwave Technol.*, 2014, 33, (3), pp. 663-669
- [41] Kim, B.G., Bae, S.H., Kim, H., et al.: 'RoF-Based Mobile Fronthaul Networks Implemented by Using DML and EML for 5G Wireless Communication Systems', *IEEE J. Lightwave Technol.*, 2018, 36, (14), pp. 2874-2881
- [42] Deng, R., He, J., Chen, M., et al.: 'Real-Time LR-DDO-OFDM Transmission System Using EML With 1024-Point FFT', *IEEE Photon. Technol. Lett.*, 2015, 27, (17), pp. 1841-1844
- [43] Hsu, D.Z., Wei, C.C., Chen, H.Y., et al.: '21 Gb/s after 100 km OFDM long-reach PON transmission using a cost-effective electro-absorption modulator', *OSA Opt. Expr.*, 2010, 18, (26), pp. 27758-27763

- [44] Giddings, R.P., Hugues-Salas, E., Tang, J.M.: 'Experimental demonstration of record high 19.125Gb/s real-time end-to-end dual-band optical OFDM transmission over 25km SMF in a simple EML-based IMDD system', *OSA Opt. Expr.*, 2012, 20, (18) pp. 20666-20679
- [45] Lin, X., Li, J., Baldemair, R., et al.: '5G New Radio: Unveiling the Essentials of the Next Generation Wireless Access Technology', *IEEE Comm. Standards Mag.*, 2019, 3, (3), pp. 30-37
- [46] Stöhr, A., Kitayama, K., Jäger, D.: 'Full-Duplex Fibre-Optic RF Subcarrier Transmission Using a Dual-Function Modulator/Photodetector', *IEEE Trans. Microw. Theory and Tech.*, 1999, 47, pp. 1338-1341
- [47] Welstand, R., Pappert, S., Sun, C., et al.: 'Dual-Function Electroabsorption Waveguide Modulator/Detector for Optoelectronic Transceiver Applications', *IEEE Photon. Technol. Lett.*, 1996, 8, 1540-1542
- [48] Garreau, A., Kazmierski, C., Chiaroni, D., et al.: '10 Gbit/s Drop and Continue Colorless Operation of a 1.5 $\mu$ m AlGaInAs Reflective Amplified Electroabsorption Modulator', *Proc. Europ. Conf. Opt. Comm., Cannes, France, Sep. 2006, We.1.6.5*
- [49] Chacinski, M., Westergren, U., Thylen, L., et al.: '50 Gb/s Modulation and/or Detection with a Travelling-Wave Electro-Absorption Transceiver', *Proc. Opt. Fiber Comm. Conf., San Diego, United States, Feb. 2008, JThA32*
- [50] Thakur, M.P., Quinlan, T.J., Bock, C., et al.: '480-Mbps, Bi-Directional, Ultra-Wideband Radio-Over-Fiber Transmission Using a 1308/1564-nm Reflective Electro-Absorption Transducer and Commercially Available VCSELs" *IEEE J. Lightwave Technol.*, 2009, 27, (3), pp. 266-272
- [51] Wu, T.H., Wu, J.P., Chiu, Y.J.: 'Novel Ultra-wideband (UWB) Photonic Generation through photodetection and crossabsorption modulation in a single Electroabsorption Modulator', *OSA Opt. Expr.*, 2010, 18, (4), pp. 3379-3384
- [52] Schrenk, B., Lazaro, J.A., Kazmierski, C., et al.: 'Colorless FSK Demodulation and Detection With Integrated Fabry-Pérot Type SOA/REAM', *IEEE Photon. Technol. Lett.*, 2010, 22, (13), pp. 1002-1004
- [53] B. Schrenk: 'Injection-Locked Coherent Reception Through Externally Modulated Laser', *IEEE J. Sel. Topics in Quantum Electron.*, 2018, 24, (2), p. 3900207
- [54] Lidoyne, O., Gallion, P., Chabran, C., et al.: 'Locking range, phase noise and power spectrum of an injection-locked semiconductor laser', *IEE Proc.*, 1990, 137, (3), pp. 147-154
- [55] Li, W., Zhu, N.H., Wang, L.X., et al.: 'Frequency-Pushing Effect in Single-Mode Diode Laser Subject to External Dual-Beam Injection', *IEEE J. Quantum Electron.*, 2010, 46, (5), pp. 796-803
- [56] Schrenk, B., Milovancev, D., Vokic, N., et al.: 'Coherent Homodyne TDMA Receiver Based on TO-can EML for 10 Gb/s OOK with <40 ns Guard Interval', *Proc. Opt. Fiber Comm. Conf., San Diego, United States, Mar. 2020, W4G.4*
- [57] Tanbun-Ek, T., Adams, L.E., Nykolak, G., et al.: 'Broad-Band Tunable Electroabsorption Modulated Laser for WDM Application', *IEEE J. Sel. Topics in Quantum Electron.*, 1997, 3, (3), pp. 960-967
- [58] Sekiguchi, S., Takabayashi, K., Hayakawa, A., et al.: '10 Gb/s Wavelength-Tunable EML with Continuous Wavelength Tuning Covering 50 GHz  $\times$  8 Channels on ITU Grid', *Proc. Opt. Fiber Comm. Conf., Anaheim, United States, Mar. 2007, OMS4*
- [59] Fabrega, J.M., Schrenk, B., Bonada, F., et al.: 'Modulated Grating Y-Structure Tunable Laser for  $\lambda$ -Routed Networks and Optical Access', *IEEE J. Sel. Topics in Quantum Electron.*, 2011, 17, pp. 1542-1551
- [60] Schrenk, B., Karinou, F.: 'Simple Laser Transmitter Pair as Polarization-Independent Coherent Homodyne Detector', *OSA Opt. Expr.*, 2019, 27, (10), pp. 13942-13950
- [61] Schrenk, B., Hofer, M., Zemen, T.: 'Analogue Receiver for Coherent Optical Analogue Radio-over-Fiber Transmission', *OSA Opt. Lett.*, 2017, 42, (16), pp. 3165-3168
- [62] Schrenk, B., Karinou, F.: 'Analogue Coherent TDMA Receiver with Fast Locking to Free-Running Optical Emitters', *IEEE J. Lightwave Technol.*, accepted for publication / available in early access.
- [63] Davis, A.W., Pettitt, M.J., King, J.P., et al.: 'Phase Diversity Techniques for Coherent Optical Receivers', *IEEE J. Lightwave Technol.*, 1987, 5, (4), pp. 561-571
- [64] Balakier, K., Fice, M.J., Ponnampalam, L., et al.: 'Foundry fabricated photonic integrated circuit optical phase lock loop', *OSA Opt. Expr.*, 2017, 25, (15), pp. 16888-16897
- [65] Pan, C., Elkashlan, M., Wang, J., et al.: 'User-Centric C-RAN Architecture for Ultra-Dense 5G Networks: Challenges and Methodologies', *IEEE Comm. Mag.*, 2017, 56, (6), pp. 14-20
- [66] Alimi, I.A., Teixeira, A.L., Monteiro, P.P.: 'Toward an Efficient C-RAN Optical Fronthaul for the Future Networks: A Tutorial on Technologies, Requirements, Challenges, and Solutions', *IEEE Comm. Surveys & Tutorials*, 2018, 20, (1), pp. 708-769
- [67] Yao, J.: 'Microwave Photonics', *IEEE J. Lightwave Technol.*, 2009, 27, (3), pp. 314-335
- [68] Parajuli, H.N., Shams, H., Guerrero Gonzalez, L., et al.: 'Experimental demonstration of multi-Gbps multi sub-bands

- FBMC transmission in mm-wave radio over a fiber system', *OSA Opt. Expr.*, 2018, 26, (6), pp. 7306-7312
- [69] Pfeiffer, T.: 'Next Generation Mobile Fronthaul and Midhaul Architectures', *IEEE/OSA J. Opt. Comm. Netw.*, 2015, 7, (11), pp. B38-B45
- [70] Liu, X., Zeng, H., Chand, N., et al.: 'Efficient Mobile Fronthaul via DSP-based Channel Aggregation', *IEEE J. Lightwave Technol.*, 2016, 34, (6), pp. 1556-1564
- [71] Rohde, H., Gottwald, E., Teixeira, A., et al.: 'Coherent Ultra Dense WDM Technology for Next Generation Optical Metro and Access Networks', *IEEE J. Lightwave Technol.*, 2014, 32, (10), pp. 2041-2052
- [72] Zhu, N.H., Zhang, H.G., Man, J.W., et al.: 'Microwave generation in an electro-absorption modulator integrated with a DFB laser subject to optical injection', *OSA Opt. Expr.*, 2009, 17, (24), pp. 22114-22123
- [73] Vacondio, F., Bertran-Pardo, O., Pointurier, Y., et al.: 'Flexible TDMA Access Optical Networks Enabled by Burst-mode Software Defined Coherent Transponders', *Proc. Europ. Conf. Opt. Comm.*, London, United Kingdom, Sep. 2013, We.1.F.2
- [74] Spano, P., Tamburrini, M., Piazzolla, S.: 'Optical FSK Modulation Using Injection-Locked Laser Diodes', *IEEE J. Lightwave Technol.*, 1989, 7, (4), pp. 726-728
- [75] Bennett, B.R., Soref, R.A., Del Alamo, J.A.: 'Carrier-Induced Change in Refractive Index of Inp, GaAs, and InGaAsP', *IEEE J. Quantum Electron.*, 1990, 26, (1), pp. 113-122
- [76] McCaulley, J.A., Donnelly, M., Vernon, M., et al.: 'Temperature dependence of the near-infrared refractive index of silicon, gallium arsenide, and indium phosphide', *APS Phys. Rev. B*, 1994, 49, (11), p. 7408
- [77] Schrenk, B., Karinou, F.: 'EML Transmitter as Coherent Monitor for Distributed Spectrum Snooping', *Proc. Europ. Conf. Opt. Comm.*, Dublin, Ireland, Sep. 2019, We.P18
- [78] Schrenk, B.: 'Synchronized Wavelength-Swept Signal Transmission and its Ability to Evade Optical Reflection Crosstalk', *OSA Opt. Lett.*, 2019, 44, (11), pp. 2771-2774
- [79] Schrenk, B., Karinou, F.: 'A Coherent Homodyne TO-Can Transceiver as Simple as an EML', *IEEE J. Lightwave Technol.*, 2019, 37, (2), pp. 555-561
- [80] Schrenk, B.: 'The EML as Analogue Radio-over-Fiber Transceiver – a Coherent Homodyne Approach', *IEEE J. Lightwave Technol.*, 2019, 37, (12), pp. 2866-2872
- [81] Schrenk, B., Milovancev, D., Vokic, N., et al.: 'Radio-over-Air with a Face-to-Face EML Transceiver Pair', *Proc. Europ. Conf. Opt. Comm.*, Dublin, Ireland, Sep. 2019, Tu.3.C.2
- [82] Schrenk, B., Karinou, F.: 'A Tandem of EMLs as Low-Cost OTDR', *Proc. Opt. Fiber Comm. Conf.*, San Diego, United States, Mar. 2019, M4G.2